

UNIVERSIDADE ESTADUAL DE CAMPINAS
SISTEMA DE BIBLIOTECAS DA UNICAMP
REPOSITÓRIO DA PRODUÇÃO CIENTÍFICA E INTELECTUAL DA UNICAMP

Versão do arquivo anexado / Version of attached file:

Versão do Editor / Published Version

Mais informações no site da editora / Further information on publisher's website:

<https://onlinelibrary.wiley.com/doi/abs/10.1002/asna.201512227>

DOI: 10.1002/asna.201512227

Direitos autorais / Publisher's copyright statement:

©2015 by Wiley-VCH Verlag. All rights reserved.

DIRETORIA DE TRATAMENTO DA INFORMAÇÃO

Cidade Universitária Zeferino Vaz Barão Geraldo

CEP 13083-970 – Campinas SP

Fone: (19) 3521-6493

<http://www.repositorio.unicamp.br>

Reviewing recent results from the Pierre Auger Observatory

C. Dobrigkeit^{1,*} for the Pierre Auger Collaboration^{2,**}

¹ Instituto de Física Gleb Wataghin, Universidade Estadual de Campinas, 13083-859 Campinas, SP, Brazil

² Observatorio Pierre Auger, Av. San Martín Norte, 304, 5613 Malargüe, Argentina

Received 2015 Sep 21, accepted 2015 Sep 26

Published online 2015 Nov 20

Key words astroparticle physics – cosmic rays – instrumentation: detectors – telescopes

The Pierre Auger Observatory addresses the most fundamental questions about the nature and origin of the highest-energy cosmic rays. The results obtained by the Auger Observatory have already led to a number of major breakthroughs in the field contributing to the advance of our understanding of these extremely energetic particles. The spectrum and the arrival direction distribution are key observables to search for sources or source regions of ultra-high energy cosmic rays, and to understand the transition from Galactic to extragalactic cosmic rays. We present the latest results on the energy spectrum, and on the studies of anisotropies performed on the ten-year dataset of arrival directions of cosmic rays at large and small angular scales. We also address the plans and motivations for the future upgrade of the Pierre Auger Observatory.

© 2015 WILEY-VCH Verlag GmbH & Co. KGaA, Weinheim

1 Introduction

The Pierre Auger Observatory is the largest cosmic-ray facility ever built (Aab et al. 2015a). Its main purpose is studying cosmic rays in the highest-energy region from 10^{17} to 10^{20} eV. The observatory is operated by an international collaboration gathering around 500 physicists from seventeen countries. It is located near the town of Malargüe (32.5° S, 69.5° W) in the province of Mendoza, Argentina, at 1400 m above sea level. This is a privileged location with an extensive and almost flat area, a clear atmosphere, and favourable weather conditions. The Galactic centre lies well in its field of view, transiting only a few degrees off its zenith.

The observatory covers an overall area of 3000 km^2 . Its main advantage is the employment of two complementary techniques for the detection of extensive air showers induced in the atmosphere by ultra-high energy cosmic rays (UHECRs) impinging on Earth. It measures the lateral distribution of air-shower particles with surface detectors on the ground, as well as the longitudinal profile of the number of shower particles, using fluorescence telescopes, through the nitrogen fluorescence light emitted along the shower axis. To that end 1600 detectors are deployed on a surface array (SD) on a 1500 m triangular grid, and a fluorescence detector (FD) with 24 telescopes overlooks the atmosphere above the SD from four sites located on the perimeter of the array. The fluorescence telescopes operate during dark, moonless nights, with a duty cycle of $\sim 13\%$, and provide an almost calorimetric measure of the shower energy. The SD operates all the time, presenting a duty cycle of almost 100% . Showers measured simultaneously with both detec-

tors are employed for establishing an energy calibration, relating the energies measured with the FD to certain shower-characteristic quantities measured with the SD. Once the energy calibration is set, it may be extended to all those showers measured with the SD. This calibration procedure is described in detail in (Aab et al. 2015a), and in (Dobrigkeit et al. 2014). The observatory is fully efficient for detection of showers with energies above 3 EeV and zenith angles up to 60° .

The construction of the Pierre Auger Observatory in its original conception was completed in 2008, and since then some enhancements have been added either exploring new detection techniques or extending its detection capability down to lower energies. Three further High-Elevation Auger Telescopes (HEAT) allow the observation of portions of the showers at higher elevation in the atmosphere. An enhancement dedicated to measuring the muon content in air showers is under construction: the Auger Muon and Infilled Ground Array (AMIGA) consists of a denser array of surface detectors, and buried scintillator detectors nearby. The denser array is comprised of 61 surface detectors at half the distance between the detectors (750 m) and deployed over an area of 23.5 km^2 in a region of the SD just in front of one of the fluorescence sites. This infilled array is overlooked by both normal and high-elevation fluorescence telescopes at that site, and allows for an extension in the detection capability of the observatory down to 10^{17} eV. The infilled array is fully efficient for showers of energy higher than 3×10^{17} eV and zenith angles up to 55° . The Auger Engineering Radio Array (AERA) explores the capabilities of detecting air showers with dual-polarization radio antennas through the signals emitted in the 30 to 80 MHz band. At the present, AERA includes 153 autonomous radio stations deployed over an area of 17 km^2 . AERA opens the poten-

* Corresponding author: carola@ifi.unicamp.br

** Full author list: http://www.auger.org/archive/authors_2015_05.html

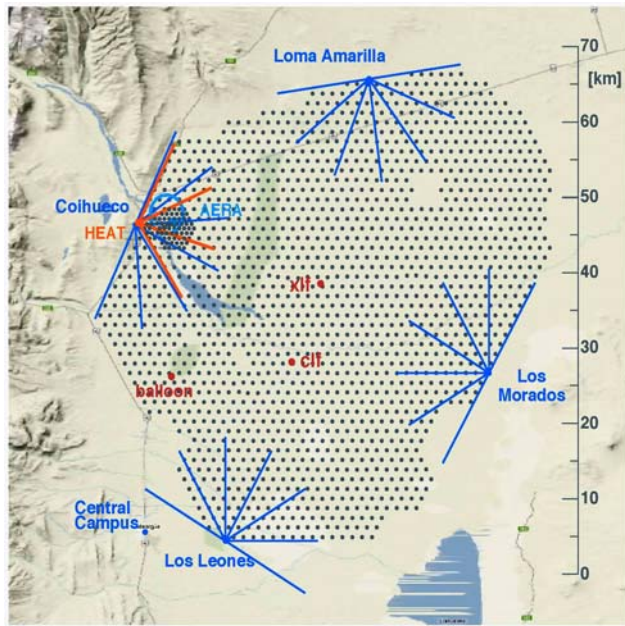


Fig. 1 The Pierre Auger Observatory. Each dot corresponds to one of the 1661 surface detector stations. The four fluorescence detector sites are also shown, with the 30° field of view of each of their six telescopes. At the Coihueco site the location of the denser array, of the AERA radio-station array, and HEAT are shown. Also depicted are the two laser facilities, CLF and XLF, near the center of the SD, as well as the balloon-launching site (Ghia et al. 2015).

tial of an independent determination of the energy scale of cosmic rays detected at the Observatory.

An extensive atmospheric monitoring is performed at the observatory site during operation of the fluorescence telescopes. The Central Laser Facility (CLF) and the eXtreme Laser Facility (XLF) are used to periodically measure the aerosol optical depths needed for the reconstruction of air showers detected by the FD. The detailed description of these detectors as well as calibration procedures can be found in Aab et al. (2015a). In Fig. 1 a schematic overview of the detector layout at the Pierre Auger Observatory is shown, with each dot corresponding to one of the 1661 surface detector stations. The four fluorescence detector sites are also shown, with the 30° field of view of each of their six telescopes. Also shown in the same figure are the locations of the AERA radio stations, the HEAT telescopes, and the two laser facilities, CLF and XLF, near the center of the SD, as well as the balloon-launching site.

2 Recent results

Measuring the energy spectrum, the mass composition, and the distribution of arrival directions of cosmic particles gives us clues about their origin and potential source(s) or source regions, which is the ultimate goal of the Pierre Auger Observatory. In its most recent publications the Pierre Auger Collaboration has presented for the first time results obtained from analyses including highly-inclined air

showers, those arriving with zenith angle between 60° and 80°. Such showers require a special procedure for reconstruction (Aab et al. 2014a). Including these inclined events allows an increase of 30 % in the exposure of the Observatory and a larger sky coverage, reaching almost 85 % of the sky from −90° to 45° in declination. The array is fully efficient for inclined events at energies above 4×10^{18} eV. Besides providing an increase of about 30 % in the number of events over the previous analyses, the inclined events are important for studies of composition, of arrival direction distributions, and also to constrain current models used to describe hadronic interactions at energies above 4×10^{18} eV, corresponding to $E_{\text{CM}} \approx 87$ TeV in proton-proton collisions.

2.1 Energy spectrum

The Pierre Auger Observatory has been operating continuously since 2004 January 1. The latest results published by the Auger Collaboration are based on various analyses of data taken over a period of ten years. In 2015 the Auger Collaboration reported the energy spectrum of cosmic rays at energies above 10^{17} eV with unprecedented precision, combining the spectra obtained from four datasets: hybrid events (those measured simultaneously with the SD and the FD), events measured by the infilled 750 m SD array, and two datasets of events measured by the 1500 m SD array, one including vertical showers (zenith angles below 60°) and the other including inclined ones (zenith angles from 60° up to 80°). The results are based on the analysis of nearly 200 000 events, and a correspondent total exposure exceeding 50 000 km² sr yr (Valiño et al. 2015). The four independent measurements of the energy spectrum are depicted in Fig. 2 (top). Systematic uncertainties in fluxes are 5.8 % and 5 % for vertical and inclined events measured with the 1500 m SD array, respectively. For the 750 m SD array, the corresponding uncertainty decreases from 14 % at $10^{17.5}$ eV to 7 % above $10^{18.5}$ eV. Following the same tendency, the uncertainty in the hybrid flux diminishes from 10 % at 10^{18} eV to less than 6 % above 10^{19} eV.

The resulting all-particle spectrum confirms two features that were reported previously by the Auger Collaboration: a hardening of the spectrum around $(4.8 \pm 0.1 \pm 0.8) \times 10^{18}$ eV, known as the “ankle”, and a flux suppression at the energy $E_s = (42.1 \pm 1.7 \pm 7.6) \times 10^{18}$ eV. These values correspond to the best fit of the all-particle spectrum shown in Fig. 2 (bottom), and the given uncertainties correspond to the statistical and systematic ones, respectively. Below the energy corresponding to the ankle, namely 4.8×10^{18} eV, the spectrum can be well described by a power law $J(E) = J_0(E/E_{\text{ankle}})^{-\gamma}$ with index $\gamma = (-3.29 \pm 0.02 \pm 0.05)$. For energies above, the spectrum can be fitted to a power law with index $(-2.60 \pm 0.02 \pm 0.10)$ including a smooth suppression at the highest energies. Above E_s , the spectrum suffers a drastic steepening, confirming the flux suppression at the highest energies. Here E_s corresponds to the energy at which the *differential* flux reduces to one-half of the value

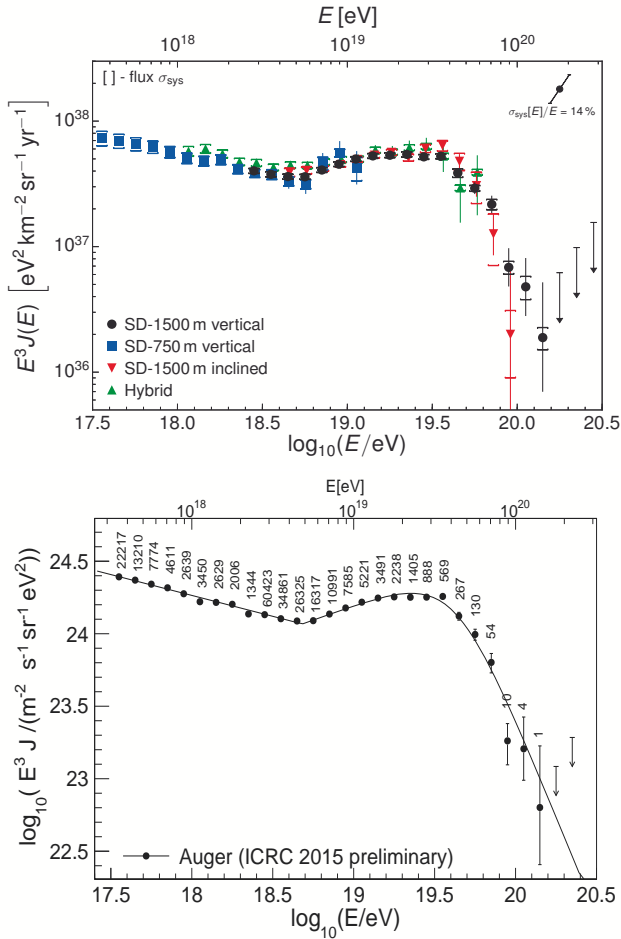


Fig. 2 The Auger energy spectra obtained from hybrid events, from SD data obtained with the 1500 m array for vertical and inclined events, and from vertical events with the infilled SD array (*top*). The combined all-particle spectrum and corresponding fit, with the number of events in each log E bin (*bottom*). The error bars represent only the statistical uncertainties. Upper limits correspond to a confidence level of 84 % (Valiño et al. 2015).

expected when extrapolating the power-law behaviour observed at energies just above the ankle.

The Auger Collaboration has also analyzed the energy spectrum with respect to a potential dependence on the declination. For this purpose it is important to take into account experimental, atmospheric, and geomagnetic effects that can possibly induce spurious modulations. Once corrected for such effects, the resulting spectra including only vertical events are shown in Fig. 3 for four declination bands. No significant departures from the all-particle spectra presented in Fig. 2 are observed, the largest deviations being less than 5 % below E_s , and less than 13 % above it.

The simplest interpretations of the two features observed in the spectrum are that the ankle is a signal of the transition from Galactic to extragalactic cosmic rays, with the first component slowly fading out, and the flux then recovering as the energy increases with the onset of the extragalactic component. On the other hand, a pos-

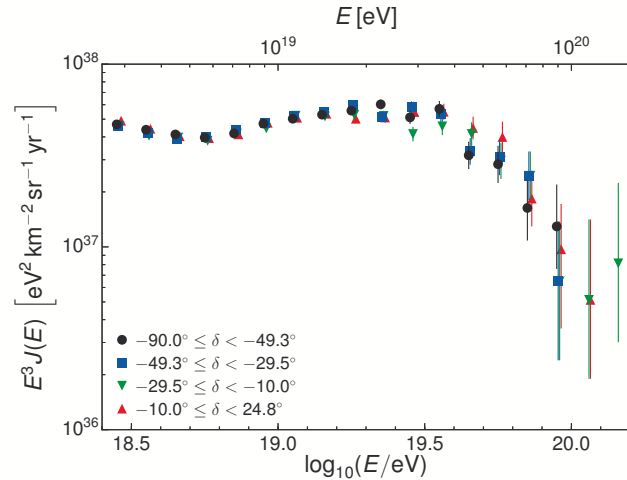


Fig. 3 Energy spectrum obtained from vertical events measured with the SD in four declination bands (Valiño et al. 2015).

sible interpretation for the suppression is that it occurs due to energy losses suffered by cosmic rays in their interactions with photons from the cosmic-microwave background radiation (CMB), a phenomenon already predicted by Greisen (1966), and, independently, by Zatsepin and Kuz'min (1966) soon after the discovery of the CMB. Following their predictions, protons on their way from their sources to Earth would suffer photo-pion interactions through the delta resonance. By the same token, cosmic nuclei could suffer photo-nuclear disintegration. Both processes would lead to protons arriving at Earth with lower energies.

Nonetheless, to fully establish the veracity of these interpretations, one should also know the mass composition of cosmic rays over the whole energy region over which the spectrum is measured. Both features can be reproduced in a model scenario in which continuously distributed sources inject protons with an energy spectrum proportional to $E^{-\beta}$, and exponentially suppressed with a scale parameter E_{cut} of the order of 10^{20} eV. A cosmological evolution of the source luminosity must also be adopted following a behavior parameterised as $(1+z)^m$. In such a scenario, a reasonably good description can be obtained assuming protons to be injected, and choosing the values $m = 5$ and $\beta = 2.35$ (Schulz et al. 2013). On the other hand, the ankle can be reproduced assuming electron-positron pairs to be produced in the interactions of protons with the CMB (Berezinsky, Gazizov & Grigorieva 2006). One notes that these interpretations rely on UHECRs being protons.

Alternatively, if one assumes that there is an upper limit in the energy to which the sources can accelerate particles depending on their charge, one is led to a description in which the observed flux suppression at the highest energies is due to a cutoff of the source spectrum rather than being an effect of energy losses during propagation. Further information about mass composition seems therefore indispensable to decide among different scenarios.

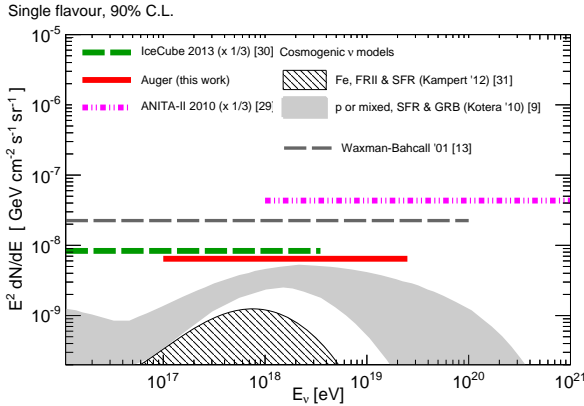


Fig. 4 Upper limit of the diffusive neutrino flux at the 90 % confidence level. Also shown are limits of other experiments and predictions of some cosmogenic neutrino models assuming heavier primary nuclei like iron, or a mixed primary composition (Aab et al. 2015b). For detailed references, see text.

The Auger Collaboration has reported results of mass composition analyses based on the evolution of the average depth of shower maximum, and its fluctuations with energy (Aab et al. 2014b, 2014c). These results were also discussed during this symposium, and are included in this volume (Molina Bueno et al. 2015). Various studies report a change in the composition from a light one at energies around $10^{18} - 10^{18.5}$ eV, becoming heavier with increasing energy, and probably being composed of intermediate nuclei such as CNO. The muon component of air showers is also sensitive to the nature of the primary particle that initiated the shower. Results of analyses published by the Auger Collaboration involving the muon component were also presented at this symposium by Molina Bueno et al. (2015), and therefore will not be repeated here.

From those mass-composition analyses, and assuming that the current models used in the simulation of hadronic interactions are a fair representation of reality, one can conclude that the primary cosmic rays are light at energies between $10^{18} - 10^{18.5}$ eV, and then become gradually heavier as their energies increase. These results are rather intriguing and cast some shadows on the simple interpretations in the scenarios mentioned above. The tendency towards a heavier composition at the highest energies reported by the Pierre Auger Collaboration seems to indicate a far more complicated scenario, and suggests the possibility that the suppression is rather a source effect. To solve this conundrum, more measurements of mass composition are needed especially extending well into the energy region of the suppression.

2.2 Neutral messengers

In various scenarios of UHECR production, photons, and neutrinos are expected to be produced either through the decay of heavier particles (the so-called top-down models) or else, and in lower quantity, as secondary particles in interactions occurring in the source environment or during

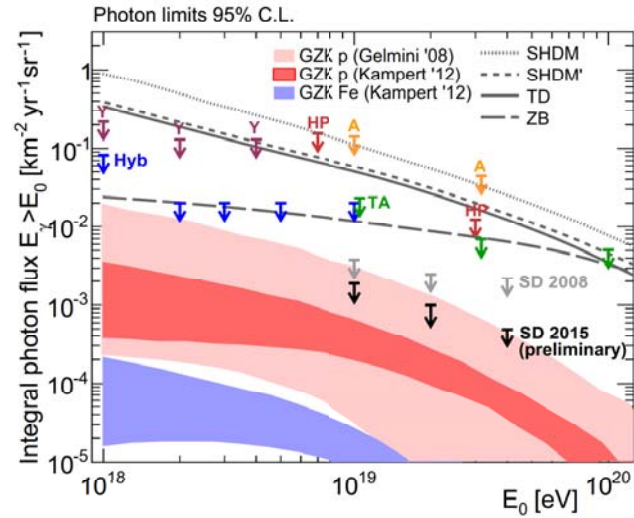


Fig. 5 Upper limits of the diffuse flux of UHE photons at the 95 % confidence level together with previous results of the Auger Collaboration (Hyb and SD), results from Telescope Array (TA), Yakutsk (Y), Haverah Park (HP), AGASA (A), and predictions from several top-down models and cosmogenic photon models (Bleve et al. 2015). For detailed references, see text.

the propagation of UHECRs. The Auger Collaboration has searched for showers initiated by UHE photons and neutrinos in the data, but no candidates were found, or unambiguously confirmed so far. This negative result strongly disfavours top-down models as a possible process of UHECR production. The results also allow the Collaboration to set upper limits on the neutrino flux (Aab et al. 2015b), which are presented in Fig. 4, and were obtained assuming that the differential neutrino flux follows a power-law spectrum E^{-2} , and a neutrino flavour ratio 1:1:1. Also shown are limits from other experiments, IceCube (Aartsen et al. 2013) and ANITA-II (Gorham et al. 2012), and predictions based on some theoretical models of cosmogenic neutrinos assuming heavier primary nuclei, either pure iron (Kampert & Unger 2012), or a mixed primary composition (Kotera, Allard & Olinto 2010). It is worth noting that the Auger Collaboration was the first air-shower experiment to set a limit below the Waxman-Bahcall bound on neutrino production in optically thin sources (Bahcall & Waxman 2001).

The latest results on the flux limit of photons (Bleve et al. 2015) are depicted in Fig. 5, presenting upper limits of the diffuse flux of UHE photons at the 95% confidence level. Also shown are previous results reported by the Auger Collaboration obtained from hybrid (Hyb) and SD events, together with results from other experiments, Telescope Array (Abu-Zayyad et al. 2013), Yakutsk (Glushkov et al. 2010), Haverah Park (Ave et al. 2000), AGASA (Shinozaki et al. 2002), and from predictions from several top-down models (Gelmini, Kalashev & Semikoz 2008; Ellis, Mayes & Nanopoulos 2006) and cosmogenic photon models (Gelmini, Kalashev & Semikoz 2008; Kampert & Unger 2012; Sarkar et al. 2011).

If there are sources in our Galaxy emitting protons up to the ankle energy, these could be detected through a flux of neutrons produced in pion photoproduction and in proton interactions. Neutron-induced air showers are indistinguishable from proton-induced ones. But being neutral, they point directly to their sources, since they do not suffer deflections due to intervening magnetic fields during their propagation. The Auger Collaboration has searched for an excess of events over small solid angles in the sky in its field of view, that could indicate a potential source. No statistically significant excess was detected (Abreu et al. 2012). An independent targeted search was also performed, combining sets of candidate sources, and additionally in the region of the Galactic centre and Galactic plane. No search resulted in significant evidence of detected neutrons (Aab et al. 2014d).

2.3 Arrival directions

The study of arrival direction distributions gives important hints for our understanding of the transition from a Galactic to an extragalactic origin of cosmic particles, and about the location of potential sources or source regions of UHECRs. The Pierre Auger Collaboration has also recently studied anisotropies both in large and small angular scales using an extended cosmic-ray data set including for the first time cosmic rays arriving with zenith angles between 60° and 80° . This inclusion allows the coverage of 85 % of the sky up to a declination of $+45^\circ$, increasing the number of cosmic-ray particles in the analyses by 30 %.

The large-scale analysis involved 70 000 events with energies above 4 EeV (4×10^{18} eV), thus in the energy region in which the detection efficiency is 100 % for inclined events (Aab et al. 2015c). Corrections for atmospheric and geomagnetic effects were taken into account, as well as the partial-sky exposure. Corrections were also applied for the small modulations in the exposure due to the varying size of the array during the construction period, as well as effects due to a small tilt of 0.2° of the array from a horizontal plane. Rayleigh analyses were done both in right ascension and in azimuthal angle, allowing one to obtain the components of a possible dipole along the equatorial plane and along the Earth's rotation axis, respectively. Assuming a general dipole distribution, the resulting dipole components were $\approx 3\%$ and $\approx 7\%$ in two energy intervals $4 \text{ EeV} < E < 8 \text{ EeV}$ and $E > 8 \text{ EeV}$, respectively, the result of highest significance being the one in the highest energy band. Assuming that the only significant contribution to the anisotropy stems from the dipole component, the results point to a dipole amplitude of 0.073 ± 0.015 for $E > 8 \text{ EeV}$ in the direction $(\alpha, \delta) = (95^\circ \pm 13^\circ, -39^\circ \pm 13^\circ)$. The sky map of the cosmic-ray flux is presented in Fig. 6 (top) applying a smoothing of 45° (Samarai et al. 2015). In the lower energy interval, the dipole was non-significant. A possible quadrupolar contribution was investigated, and also turned out not to be significant. The observed anisotropy could be caused by an inhomogeneity in the source distribution nearby.

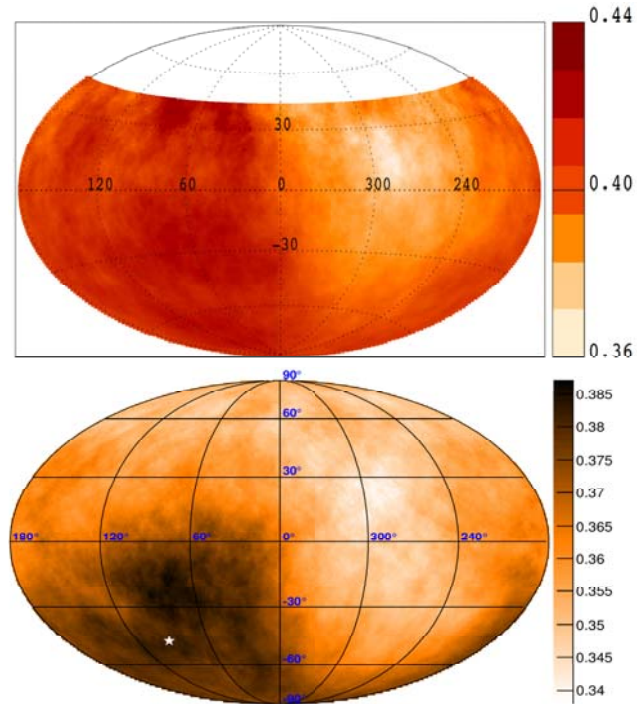


Fig. 6 *Top:* sky map of the cosmic-ray flux above 8 EeV with a smoothing of 45° (Samarai et al. 2015). *Bottom:* sky map of the full-sky cosmic flux above 10 EeV using data from both Auger and TA, with a smoothing of 60° . The direction of the reconstructed dipole is represented by the white star (Deligny et al. 2015). Both fluxes are shown in equatorial coordinates, and expressed in units of $\text{km}^{-2} \text{sr}^{-1} \text{yr}^{-1}$.

Upper limits for the dipolar and quadrupolar amplitudes have also been reported as result of a joint analysis of data of the Pierre Auger and Telescope Array (TA) Collaborations covering the full sky (Aab et al. 2014e; Deligny et al. 2015). Thanks to the combination of data, the measurement of the dipole moment does not depend on any previous assumption involving the cosmic-ray flux. The latest result of the spherical harmonic analysis of the full-sky cosmic flux as obtained from 17 000 events measured by the Auger Observatory and 2500 events measured by TA is depicted in Fig. 6 (bottom) with a 60° smoothing. That analysis results a dipole amplitude of 0.065 ± 0.019 for $E > 10 \text{ EeV}$ in the direction $(\alpha, \delta) = (93^\circ \pm 24^\circ, -46^\circ \pm 18^\circ)$ (Deligny et al. 2015). That dipole moment has a chance probability of 5×10^{-3} , and was the only multipole to deviate from fluctuations of an isotropic flux at the 99% confidence level.

The amplitude of the first harmonic in right ascension as well as its phase were also evaluated for cosmic rays with energies between 0.02 and 20 EeV, a crucial energy interval for studying the transition from Galactic to extragalactic cosmic rays. The values for the amplitudes are within those expected from isotropy at the 99 % confidence level with the exception of that in the highest-energy bin. The phases show an evolution with energy, pointing to the Galactic centre for energies below 1 EeV and turning to the anti-Galactic centre at the highest energies within the uncertainties, thus

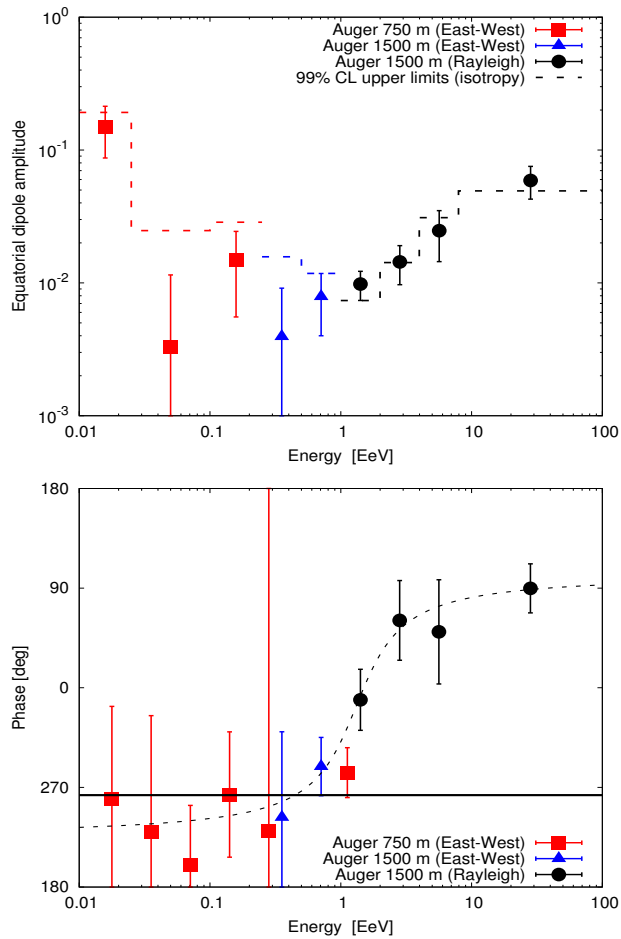


Fig. 7 Equatorial dipole amplitude (*top*) and phase of the first harmonic in the arrival direction distribution (*bottom*) as a function of energy from data up to 2011 (Sidelnik et al. 2013).

confirming the results reported in (Sidelnik et al. 2013). The results of the analysis are shown in Fig. 7. Currently a prescribed test is under way to evaluate the significance of these results. The prescribed exposure is expected to be attained in mid-2015.

Arrival-direction distributions were also thoroughly scrutinised to look for potential deviations from isotropy at small angular scales (Aab et al. 2015d). The correlation analysis with active galactic nuclei (AGNs) from the Véron-Cetty and Véron catalogue (VCV) (Véron-Cetty & Véron 2006) was updated for the larger set of events. Searches for excess arrivals from the Galactic centre and equatorial plane, from the Super-Galactic equatorial plane, and from circular regions in the sky, in particular around Centaurus A (Cen A), were done. The most significant excess after a “blind” search for *localised* excesses was found at an energy threshold of 54 EeV in a radius 12° around Cen A, with a post-trial probability of 69 %. The corresponding sky map of significances of overdensities in 12° circular windows is presented in Fig. 8 (Aab et al. 2015d) in Galactic coordinates.

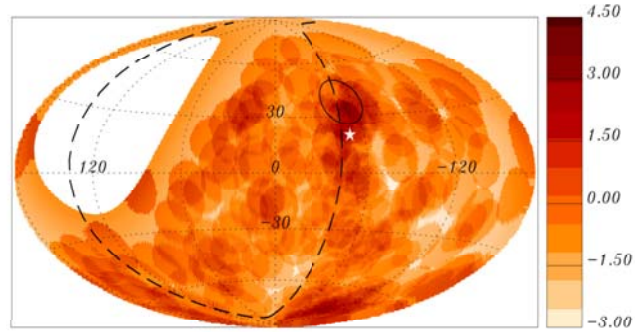


Fig. 8 Map in Galactic coordinates of the significances of overdensities in 12° angular windows for events with $E \geq 54$ EeV. The circle shows the angular window of highest significance. The dashed line indicates the Super-Galactic Plane. The direction of Centaurus A is represented by the white star (Aab et al. 2015d).

Furthermore, the two-point correlation distribution was explored, as well as correlations with directions of astrophysical objects in the 2MRS and Swift-BAT catalogues, and radiogalaxies with jets and lobes. These three catalogues consist of samples that are quite complementary in their capability to trace and identify cosmic-ray sources. Normal galaxies in the 2MRS catalogue may trace the locations of gamma-ray bursts, and fast spinning new-born pulsars. X-rays observed with Swift-BAT identify AGNs hosted by spiral galaxies, while observed radio emissions select extended jets and radio lobes hosted mainly by elliptical galaxies. In most of these analyses, scans were performed in energy threshold and over other parameters to search for evidence of anisotropy, resulting in some remarkable correlations. Nevertheless, after penalizing for the number of trials, all correlations dropped to small significance, and no significant indication of anisotropy was found. This is by itself a remarkable outcome, especially considering that the analyses involved 600 particles with energies above 40 EeV, and a total exposure of $66\,450 \text{ km}^2 \text{ sr yr}$, more than double that of the previous analyses.

It is worth mentioning the two results of highest significance. The first stems from a search for *cross-correlations* of cosmic-ray arrival directions and the direction of Cen A. The most significant result of that cross-correlation search was obtained for events with $E > 58$ EeV in a circular window of 15° around Cen A, with a 1.4 % probability of arising by chance from an isotropic distribution. The second significant result refers to the correlation with SWIFT AGNs lying within 130 Mpc, with luminosity above $10^{44} \text{ erg s}^{-1}$. In this analysis the highest significance was obtained for events above 58 EeV, for an angular window of 18° . The absence of a strong indication of anisotropy is potentially indicating that the number of sources is larger than estimated, and more uniformly distributed in the sky.

3 Conclusions

The data taken with the Pierre Auger Observatory have contributed to a major advance in the understanding of UHECRs. The flux suppression is established unambiguously, and although compatible with the predicted GZK effect, it could also be caused by an exhaustion of the acceleration capability of the cosmic-ray source(s). Strong upper limits on the photon and neutrino fluxes disfavour top-down models for the production of UHECRs. Results of mass-composition studies report on the composition changing from a light one at energies around $10^{18} - 10^{18.5}$ eV becoming heavier with increasing energy, and probably being composed of intermediate nuclei (CNO).

The arrival direction distributions have proven to be essentially isotropic, with only a few exceptions, like the indication of a dipole component at energies exceeding 8 EeV and the remarkable evolution of the phase of the first harmonic, changing from pointing to the Galactic centre to the Galactic anticentre with increasing energy.

When viewing these results in a more global perspective, one notes that they can be interpreted in the light of different scenarios. To distinguish among those requires improving the sensitivity of the Auger Observatory for measurements of mass composition. Therefore the Auger Collaboration is proposing an upgrade with additional detectors, and an extension of its operation until 2024. The main upgrade will be the installation of 4 m^2 scintillator detectors on top of the existing surface detectors, aiming a better distinguishability of the electromagnetic and muonic components of air showers, and thus providing information about the composition of the primary particles. The upgrade also includes the substitution of the current electronics allowing for an improved performance, the completion of the array of the AMIGA muon detectors, and the extension of the duty cycle of the fluorescence telescopes by allowing measurements during nights with more background light. With this increased capability and higher composition sensitivity, the Auger Observatory will provide rich measurements that will be able to address in depth the questions of the origin and the nature of UHECRs.

Acknowledgements. The successful installation, commissioning, and operation of the Pierre Auger Observatory would not have been possible without the strong commitment and effort from the technical and administrative staff in Malargüe. The author acknowledges the financial support from the Fundação de Amparo à Pesquisa do Estado de São Paulo (FAPESP) through grant 2010/07359-6 and also from the Conselho Nacional de Desenvolvimento Científico e Tecnológico (CNPq) in Brazil.

References

- Aab, A., Abreu, P., Aglietta, M., et al. (The Pierre Auger Collaboration) 2014a, JCAP, 08, 019
 Aab, A., Abreu, P., Aglietta, M., et al. (The Pierre Auger Collaboration) 2014b, Phys. Rev. D, 90, 122005

- Aab, A., Abreu, P., Aglietta, M., et al. (The Pierre Auger Collaboration) 2014c, Phys. Rev. D, 90, 122006
 Aab, A., Abreu, P., Aglietta, M., et al. (The Pierre Auger Collaboration) 2014d, ApJ, 780, L34
 Aab, A., Abreu, P., Aglietta, M., et al. (The Pierre Auger Collaboration and Telescope Array Collaboration) 2014e, ApJ, 794, 172
 Aab, A., Abreu, P., Aglietta, M., et al. (The Pierre Auger Collaboration) 2015a, to appear in Astropart. Phys.
 Aab, A., Abreu, P., Aglietta, M., et al. (The Pierre Auger Collaboration) 2015b, Phys. Rev. D, 91, 092008
 Aab, A., Abreu, P., Aglietta, M., et al. (The Pierre Auger Collaboration) 2015c, ApJ, 802, 111
 Aab, A., Abreu, P., Aglietta, M., et al. (The Pierre Auger Collaboration) 2015d, ApJ, 804, 15
 Aartsen, M. G., Abbasi, R., Ackermann, M., et al. (IceCube Collaboration) 2013, Phys. Rev. D, 88, 112008
 Abreu, P., Aglietta, M., Ahlers, M., et al. (The Pierre Auger Collaboration) 2012, ApJ, 760, 148
 Abu-Zayyad, T., Aida, R., Allen, M., et al. (Telescope Array Collaboration) 2013, Phys. Rev. D, 88, 112005
 Ave, M., Hinton, J. A., Vázquez, R. A., Watson, A. A., & Zas, E. 2000, Phys. Rev. Lett., 85, 2244
 Bahcall, J., & Waxman, E. 2001, Phys. Rev. D, 64, 023002
 Bleve, C. for the Pierre Auger Collaboration 2015, PoS(ICRC 2015)1103
 Berezhinsky, V., Gazizov, G., Grigorieva, S. 2006, Phys. Rev. D, 74, 043005
 Deligny, O. for the Pierre Auger Collaboration and Telescope Array Collaboration: 2015, PoS(ICRC2015)395
 Dobrigkeit, C. and the Pierre Auger Collaboration 2014, Astron. Nachr., 335, 573
 Ellis, J., Mayes, V. E., & Nanopoulos, D. V. 2006, Phys. Rev. D, 74, 115003
 Gelmini, G., Kalashev, O., & Semikoz, D. 2008, JETP, 106, 1061
 Ghia, P. L. for the Pierre Auger Collaboration: 2015, to appear in PoS(ICRC2015)
 Glushkov, A. V., Makarov, I. T., Pravdin, M. I., & Sleptsov, I. E. (Yakutsk EAS Array) 2010, Phys. Rev. D, 82, 041101
 Gorham, P. W., Allison, P., Baughman, B. M., et al. (ANITA Collaboration) 2012, Phys. Rev. D, 85, 049901(E)
 Greisen, K. 1966, Phys. Rev. Lett., 16, 748
 Kampert, K. -H., & Unger, M. 2012, Astropart. Phys., 35, 660
 Kotera, K., Allard, D., & Olinto, A. V. 2010, JCAP, 10, 013
 Molina Bueno, L. for the Pierre Auger Collaboration 2015, this volume
 Samarai, I. A. for the Pierre Auger Collaboration 2015, PoS(ICRC 2015)372
 Sarkar, B., Kampert, K.-H., Kulbartz, J., et al. 2011, Proc. 32nd ICRC, 2, 198
 Shinozaki, K., Chikawa, M., Fukushima, M., et al. 2002, ApJ, 571, L117
 Schulz, A. for the Pierre Auger Collaboration 2013, Proc. 33rd ICRC (ICRC2013-0769)
 Sidelnik, I. for the Pierre Auger Collaboration 2013, Proc. 33rd ICRC (ICRC2013-0739)
 Valiño, I. for the Pierre Auger Collaboration 2015, PoS(ICRC 2015)271
 Véron-Cetty, M.-P. & Véron, P. 2006, A&A, 445, 773
 Zatsepin, G. T., & Kuz'min, V. A. 1966, JETPL, 4, 78